Multi-Mode Circular Dichroism in N-Fold Rotational Symmetric Metamaterials

Shihao Li
University of Shanghai for Science and Technology
Kejian Chen (ee.kjchen@gmail.com)
University of Shanghai for Science and Technology https://orcid.org/0000-0003-3036-9274
Yeli Xu
University of Shanghai for Science and Technology
Yan Chen
University of Shanghai for Science and Technology

Research Article

Keywords: Chiral metamaterial, Circular dichroism, Multi-mode, Absorption

Posted Date: July 7th, 2021

DOI: https://doi.org/10.21203/rs.3.rs-563812/v1

Version of Record: A version of this preprint was published at Optical and Quantum Electronics on December 10th, 2021. See the published version at https://doi.org/10.1007/s11082-021-03432-7.

Abstract

In this article, the effects of the rotation angle between upper and lower n-fold rotational symmetric nano-structures are studied. Various modes of circular dichroism (single wavelength band, dual-wavelength bands, and more than two wavelength bands) in the wavelength band from 3.3 to 5 μm are realized. Absorption up to 0.994 and absorptive circular dichroism up to 0.867 are observed. Meanwhile, sensitivity of circular dichroism to the rotation angle and reconfigure strategy for opposite responses has been discussed. Based on Born-Kuhn model, physical mechanism of mode's switching is explained with charge distributions. The multi-mode chiroptical responses in mid-infrared band and the variety of design strategies have potential applications in the field of thermal remote sensing detection and tunable multi-band chiral devices.

1. Introduction

Metamaterial is an artificial material with many electromagnetic properties that do not exist in nature, such as perfect absorption (Chen, et al. 2020; Landy, et al. 2008; X. Zhang, et al. 2020), negative refraction (Valentine, et al. 2008), electromagnetically induced transparency-like (Xu, et al. 2019). It has provided excellent solutions for modulators, sensors, etc. in recent decades (Bu, et al. 2016). When metamaterials have chiral properties, such as giant optical activity; circular dichroism; negative refractive index and etc. (Cheng, et al. 2016; Hannam, et al. 2014; M. Li, et al. 2014; Z. Li, et al. 2013), they can be called chiral metamaterials. Chiral metamaterials have significant improvement in chiral parameters compared with natural chiral materials because of their strong electromagnetic coupling. Therefore, chiral metamaterials have been widely used to enhance chiral signals in molecular analysis, bio-sensor, chiral signal switch, or occasions with chiral signals (X. Ma, et al. 2017; Yoo and Park 2019). As a typical phenomenon of chirality, circular dichroism (CD) is used to characterize the different electromagnetic responses of materials between left-hand circularly polarized (LCP) waves and right-handed polarized (RCP) waves. And CD has been widely utilized in protein structure examining, nanostructural analyzing, medicine detecting, etc. (Berova, et al. 2000; Ranjbar and Gill 2009).

Bi-layer structures are often used in the studies of chiral metamaterials (Kaya 2014; Kaya, et al. 2017; Xiaolong Ma, et al. 2016; Yan, et al. 2017; Zhou, et al. 2012). Some of those works replacing the material of the dielectric layers(Kaya, et al. 2017; Yan, et al. 2017; Zhou, et al. 2012), changing some geometric parameters of the structures(Kaya, et al. 2017; Liu, et al. 2019; Xiaolong Ma, et al. 2016), or adjusting the incident angle of circularly polarized waves(Kaya 2014) in order to modulate the responses of metamaterial to circularly polarized waves. As far as we know, in similar metamaterials, there are only a few papers (Liang, et al. 2021; Wu, et al. 2013) have discussed the relative angle between the upper and lower layers. In this paper, relative rotation angles between two layers are able to realize various CD responses without changing the structure's size and material properties has been further studied. And by using specific reconfiguration methods, the polarization direction of the response and the sensitivity of the responses to the rotation angle can be adjusted.

In this article, the effect of the rotation angle on different rotational symmetric metamaterials has been studied in mid-infrared region. As a result, multi-mode CD responses; reconfigure strategy for opposite CD responses; sensitivity of the CD spectra to the rotation angle; and selective absorption are realized. Because of the atmospheric transparent windows, molecular vibration fingerprints, and attractive plasma resonances in mid-infrared region(Stanley 2012; Xinghui Yin, et al. 2015), this work will benefit the designing of n-fold chiroptical devices and has potential applications in thermal remote sensing detection.

2. Design And Simulation

With the fold of rotational symmetry increase, the sensitivity of the CD responses to the rotation angle disappears gradually. Since the responses of five-fold rotational symmetric metamaterial (Type N5) to the rotation angle have both sensitive and insensitive wavelength band, as shown in Fig. 3(b)), so it is selected to be illustrated in Fig. 1(a)-(c). Every unit of the metamaterial, marked by dotted box in the figure, is composed of a silicon dioxide substrate and two vertically placed multiple rotational symmetric gold nano-structures. A polymer film is inserted between those two nano-structures. The entire unit is periodically expanded along the x and y directions with the same period of p. The front and side views of the unit are shown in Fig. 1(b) and Fig. 1(c) respectively. As shown in Fig. 1(b), the rotation angle of the upper nano-structure is θ (counterclockwise). The length of the blades is l_2 and the side length of the center pentagon is l_1. The line width of the nano-structures is w. As shown in Fig. 1(c), the thickness of polymer film, silicon dioxide substrate, and nano-structures are h_1, h_2, and h_3 respectively. As shown in Fig. 1(d), different types and different fold of rotational symmetric units which will be discussed next are illustrated, and some parameters (if not specifically optimized) are unchanged as Type N5: line width; thickness of every material; period of units; length of the blades; and the perimeter of the center polygons. In addition, two reconfigure strategies for opposite responses and more flexible designs are marked by dashed lines in Fig. 1(d).

The n-fold rotational symmetry refers to the symmetry that the structure completely coincides with itself after the structure rotates 360°/n around the axis of rotation. It should be noted that the rotational symmetry mentioned in this paper refers to each layer of gold structure in the unit (as shown in Fig. 1(b)), not the whole metamaterial after periodic expansion (as shown in Fig. 1(a)).

In this paper, the metamaterials are designed and optimized by CST Microwave Studio. The boundary condition is set to unit cell and the incident waves are set to circular polarization. The direction of incidence is opposite to the z-axis. In order to obtain CD responses in the mid-infrared band, some parameters are optimized as follows: l_1=1.2 μm; l_2=1 μm; w=200 nm; p=4 μm; h_1=1.2 μm; h_2=100 nm; h_3=200 nm; and Gap=1 μm. The refractive index (RI) of polymer film is set to 1.35 (PTFE) (Saadeldin, et al. 2019). The optical constants of gold has been set from Johnson and Christy's data (Johnson and Christy 1972). The RI of silicon dioxide has been set to 1.4 (Liu, et al. 2019).

3. Results And Analysis

In order to discuss the modulation effect of the rotation angle on the transmission spectra more clearly, Type N4 with rotation angle of 0°, 10°, 40°, and 80° are demonstrated in Fig. 2. Here, t_{RCP} and t_{LCP} represent the co-polarized transmission coefficient of RCP and LCP waves respectively. When the rotation angle is set to 0° (i.e., Fig. 2(a)), significant asymmetric transmission can be observed in short wavelength band (3.3-3.95 μm), middle wavelength band (3.95-4.26 μm), and long wavelength band (4.26-5 μm). When the rotation angle is set to 10° (Fig. 2(b)), a large asymmetric transmission can be observed in the middle and long wavelength bands. When the rotation angle is set to 40° (Fig. 2(c)), asymmetric transmission can be observed only in middle wavelength band. And when the rotation angle is set to 80° (Fig. 2(d)), strong asymmetric transmission can be seen in short and middle wavelength bands. It should be noted that when the wavelength is less than 3.7 μm, there is nearly no asymmetric transmission in the metamaterial of Type N4.

To further investigate the modulation effect of rotation angle on chirality, the asymmetric transmission has been assessed by the CD ($CD= |t_{RCP}|^2-|t_{LCP}|^2$)(Jing, et al. 2018; S. Li, et al. 2020; Z. Wang, et al. 2017). As much as 0.609, 0.843, and 0.727 of the CD responses can be reached in three wavelength bands respectively. The CD spectra of four different rotation angles are shown in Fig. 2(e), where four different combinations of CD response in transmission spectra are marked as Mode 1, Mode 2, Mode 3, and Mode 4. Since the rotation period of the proposed metamaterial is 90°, the corresponding change of CD responses under the rotation angle from 0° to 90° have been simulated in Fig. 2(f), where the four modes mentioned before are marked by dash lines in the figure. This simulation can help to fully discover the impact of rotation angle on CD spectrum. It can be seen that when the rotation angle is adjusted periodically, the modes of proposed metamaterial can be switched cyclically.

As shown in Fig. 3(a), different folds of rotational symmetric structures are further studied. CD responses of three-fold rotational symmetric nano-structure can be modulated with the changing of rotation angle, which is same as Type N4. Five-fold rotational symmetry, as shown as Type N5, it can be observed that the CD responses in the short wavelength band can be modulated by rotation angle which is like Type N3 and Type N4. However, the CD responses in middle and long wavelength band will not be modulated. So, the responses which are not able to be modulated are defined as constant responses and the responses able to be modulated by rotation angle can be defined as switchable responses. To further investigate the relationship between the fold of rotational symmetry and CD responses, the CD spectra of the nano-structures with six and eight fold of rotational symmetry have been simulated, as shown in Fig. 3(c) and (d), where the CD spectra are almost unchanged with different rotation angles.

Therefore, with the fold of rotational symmetry increasing, the modulation effect of the rotation angle on the CD spectra will disappear gradually. In the wavelength band between 3.3 to 5 μm, rotation angle cannot change the CD spectra effectively when the fold of rotational symmetry exceeds five.

Selective absorption of circularly polarized waves is realized in this paper, as shown in Fig. 4. The absorption of LCP and RCP waves (A_{LCP} and A_{RCP}) (Cao, et al. 2013; Ouyang, et al. 2018; L. Wang, et al. 2019)can be calculated as:

$$A_{LCP} = 1 - R_{RL} - R_{LL} - T_{RL} - T_{LL} \quad (1)$$
$$A_{RCP} = 1 - R_{LR} - R_{RR} - T_{LR} - T_{RR} \quad (2)$$

Here, the R_{RL} (R_{LR}) is the cross-polarized reflectance of LCP (RCP) wave, and R_{LL}(R_{RR}) is the co-polarized reflectance of LCP (RCP) wave. The T_{RL} (T_{LR}) is the cross-polarized transmittance of LCP (RCP) wave, and T_{LL}(T_{RR}) is the co-polarized transmittance of LCP (RCP) wave.

The parameters of the different fold of rotational symmetric nano-structures are optimized to obtain their high selective absorption. Absorption of RCP waves can obtain 0.650, 0.987, 0.973, and 0.994 in Fig. 4(a), (b), (d), and (e) respectively. Absorption of LCP waves can obtain 0.915 in Fig. 4(c). Meanwhile, absorptive circular dichroism (CD_{Ab}) spectra, which is calculated by $CD_{Ab} = A_{RCP} - A_{LCP}$, are used to discuss the selective absorption of circularly polarized waves. Here, A_{RCP} (A_{LCP}) is the absorption of RCP (LCP) waves. As shown in Fig. 4(f), relatively high CD_{Ab} up to 0.867 is observed in Type N4. It should be noted that the absorption in Type N3, Type N4, and Type N5 can also be modulated by rotation angle which same as Fig. 3. So it is not being discussed in Fig. 4.

In addition, two reconfigure strategies are studied for more flexible designs. For Type N4S1 shown in Fig. 5, the direction of blades in both layers are different from Type N4, when the upper nano-structure is rotated clockwise (θ<0°), CD spectra are shown in Fig. 5(a), opposite to Fig. 2(e). Similarly, Mode -1, Mode -2, Mode -3, and Mode -4 are used to mark the occasions for rotation angles of 0°, -10°, -40°, and -80° respectively.

By changing the direction of blades in upper layer's nano-structure of Type N4 only, a unit as Type N4S2 shown in Fig. 5 has been investigated. Metamaterial of this design has significantly different CD spectra as shown in Fig. 5(b). Following the previous discusses, four different modes, three wavelength bands; short and middle wavelength bands; single wavelength band; middle and long wavelength bands, are analyzed in the figure corresponding to the rotation angles of 0°, 10°, 30°, and 80° respectively. It should be noted that different fold of rotational symmetric nano-structures which are discussed in Fig. 3 and 4 are able to follow these two reconfigure strategies for more different responses.

To explain the underlying physical mechanism of the proposed metamaterial, the charge distribution of three different modes at middle and long wavelength bands are simulated, as shown in Fig. 6. For Mode 1, when the metamaterial is excited by RCP waves at 4.04 μm, the local electric dipoles in the two horizontal nano-rods of lower layer are mainly left pointing and both of the vertical nano-rods of the lower layer have local electric dipoles pointing upward. Similarly, local electric dipoles in the upper layer are pointing right in the horizontal nano-rods and pointing upward in the vertical nano-rods. To simplify the

analysis, equivalent electric dipoles (M. Zhang, et al. 2018) have been provided as a reference and marked with solid arrows. It can be observed that the angle between the two equivalent electric dipoles is obtuse. For a Born–Kuhn model (X. Yin, et al. 2013), those two dipoles with an obtuse angle between them can form a bonding mode. In Mode 1, it can be found that the equivalent electric dipoles of the upper and lower layers are parallel when the charge distribution excited by LCP waves. That is, from the Born–Kuhn model, those two dipoles with the same pointing direction can form an antibonding mode.

To explain why modes switching can be implemented by angle rotation in the proposed metamaterial, the charge distribution at 4.58 μm of Mode 2 and Mode 3 are studied. Under the excitation of different circularly polarized waves, the local electric dipoles of Mode 2 at 4.58 μm build two different hybrid modes and the local electric dipoles of Mode 3 at 4.58 μm build two bonding modes, where the former one has strong CD response, but the latter one almost has no CD response. Furthermore, same method is used to analysis Type N8, it is found that the rotation angle between upper and lower nano-structures is not enough to change the hybrid modes. And the same hybrid modes lead to the insensitivity of the CD spectra to the rotation angle.

In plasma resonances excited by electromagnetic waves, bonding mode has lower resonance energy than antibonding mode, similar to molecular orbital theory (Q. Li and Zhang 2016; Prodan and Nordlander 2004). More specifically, the phenomenon that bonding modes have higher transmission coefficient than antibonding modes' as shown in Fig. 2 is consistent with the theories. In a summary, the hybrid mode excited by different circularly polarized waves can be adjusted by changing the rotation angle. The CD responses are very weak when the same hybrid modes are excited by different circularly polarized waves. Otherwise, if different hybrid modes excited by different circularly polarized waves, the relatively strong CD responses will appear.

It should be noted that when the rotation angle is 0°, the separate two layer of gold structure is no longer 3D chiral. However, each layer of gold structure is placed on a substrate of different thicknesses and different materials, and the gold structure of lower layer is wrapped by polymer film. The whole metamaterial unit (gold structure-polymer-gold structure wrapped by polymer-silica) is still 3D chiral(Arteaga, et al. 2016).

To reveal the advantages of this work more completely, a compassion table is established (Table. 1). As for transmitted CD, it can be seen that in the series of rotational symmetric metamaterials we discussed, different types possess different maximum transmitted CD and different number of modes can be modulated. Among the different types mentioned in this article, Type N4 has the largest number of modes and can achieve the strongest transmitted circular dichroism response. And through the reconfigure strategies which are proposed in Fig. 5, much more modes of transmitted CD can be realized. As for absorptive CD, it can also be found that strong absorptive CD are realized in Type N4 which is relatively high in the similar chiral absorbers(M. Li, et al. 2014; L. Wang, et al. 2019).

Table. 1 Some types mentioned in this work and comparison with some other chiral metamaterials

Metamaterial	Number of modes	Single wavelength band	Dual-wavelength bands	Triple-wavelength bands or more	Transmitted circular dichroism	Absorptive circular dichroism
(Yan, et al. 2017)	1	√			0.75	
(Cao, et al. 2014)	1			√	0.17	
(M. Li, et al. 2014)	1	√				0.76
(L. Wang, et al. 2019)	3		√*			0.79
Type N3	3	√	√	√	0.75	0.49
Type N4	4	√	√*	√	0.84	0.87
Type N5	3		√	√*	0.54	0.57
Type N6	1			√	0.63	0.70
Type N8	1			√	0.74	0.77

* More than one mode and all of them are dual-wavelength bands (triple-wavelength bands or more).

Declarations

Funding (This research was funded by the National Natural Science Foundation of China, grant number 61205095 and Shanghai Young College Teacher Develop funding schemes, grant number slg11006.)

Conflicts of interest/Competing interests (Not applicable)

Availability of data and material (Data transparency)

Code availability (Not applicable)

Author contributions (Conceptualization, S.L.; methodology, S.L.; formal analysis, S.L. Y.X., Y.C.; investigation, S.L.; data curation, S.L.; writing—original draft preparation, S.L.; writing—review and editing, S.L., K.C., Y.X., Y.C.; visualization, S.L., Y.X., Y.C.; supervision, K.C.; All authors have read and agreed to the published version of the manuscript.)

Acknowledgements

This work was supported in part by the National Natural Science Foundation of China under Grants 61205095, in part by the Shanghai Young College Teacher Develop funding schemes under Grant slg11006. We also thank Dr. Y.G. Du and Ms. T. Bu for their help

Conclusion

In a summary, a series of n-fold rotational symmetric metamaterials are studied in this paper. By changing the rotation angle between the upper and lower nano-structures, various modes of CD responses are realized. Meanwhile, reconfigure strategy for opposite CD responses, sensitivity of CD spectra to rotation angle, and selective absorption are studied in this work. The multi-mode chiroptical responses and the variety of designs and modulation strategies in mid-infrared have proved that this work is beneficial to the applications of thermal remote sensing detection; molecular structure detection; and bio-sensing.

References

1. ·O. Arteaga, J., Sancho-Parramon, S., Nichols, B.M., Maoz, A., Canillas, S., Bosch, G., Markovich: and B. Kahr. Relation between 2D/3D chirality and the appearance of chiroptical effects in real nanostructures. Opt. Express **24**(3), 2242–2252 (2016)
2. ·N. Berova, K., Nakanishi, Woody, R.W.: Circular dichroism: principles and applications. John Wiley & Sons (2000)
3. ·T. Bu, K., Chen, H., Liu, J., Liu, Z., Hong, Zhuang, S.: Location-dependent metamaterials in terahertz range for reconfiguration purposes. Photonics Res. **4**(3), 122–125 (2016)
4. ·T. Cao, C., Wei, Zhang, L.: Modeling of multi-band circular dichroism using metal/dielectric/metal achiral metamaterials. Optical Materials Express **4**(8), 1526–1534 (2014)
5. ·T. Cao, L., Zhang, R.E., Simpson, C., Wei: and M. J. Cryan. Strongly tunable circular dichroism in gammadion chiral phase-change metamaterials. Opt. Express **21**(23), 27841–27851 (2013)
6. ·K. Chen, X., Zhang, S., Li, Z., Lu, M., Chang, Y., Wei, Y.J., Fu, Q., Feng, L., Li, Zhuang, S.: Switchable 3D printed microwave metamaterial absorbers by mechanical rotation control. J. Phys. D: Appl. Phys. **53**(30), 305105 (2020)
7. ·Y., Z., Cheng, Y.L., Yang, Y.J., Zhou, Z., Zhang, X.S., Mao: and R. Z. Gong. Complementary Y-shaped chiral metamaterial with giant optical activity and circular dichroism simultaneously for terahertz waves. J. Mod. Opt. **63**(17), 1675–1680 (2016)
8. ·K. Hannam, D.A., Powell, I.V., Shadrivov: and Y. S. Kivshar. Broadband chiral metamaterials with large optical activity. Phys. Rev. B **89**(12), 125105 (2014)
9. ·L. Jing, Z., Wang, B., Zheng, H., Wang, Y., Yang, L., Shen, W., Yin, E., Li: and H. Chen. Kirigami metamaterials for reconfigurable toroidal circular dichroism. NPG Asia Mater. **10**(9), 888–898 (2018)
10. ·P, B., Johnson, Christy, R.W.: Optical Constants of the Noble Metals. Phys. Rev. B **6**(12), 4370–4379 (1972)
11. ·S, K.: Circular dichroism from windmill-shaped planar structures operating in mid-infrared regime. Optical Materials Express **4**(11), 2332–2339 (2014)
12. ·S. Kaya, M., Turkmen, Topaktas, O.: Design of planar chiral metamaterials for near-infrared regime. Appl. Phys. A **123**(1), 109 (2017)

13. ·N, I., Landy, S., Sajuyigbe, J.J., Mock, D.R., Smith: and W. J. Padilla. Perfect metamaterial absorber. Phys. Rev. Lett. **100**(20), 207402 (2008)
14. ·M. Li, L., Guo, J., Dong, Yang, H.: An ultra-thin chiral metamaterial absorber with high selectivity for LCP and RCP waves. J. Phys. D: Appl. Phys. **47**(18), 185102 (2014)
15. Li, ·Q., Zhang, Z.: Bonding and Anti-bonding Modes of Plasmon Coupling Effects in TiO2-Ag Core-shell Dimers. Sci Rep **6**, 19433 (2016)
16. Li, ·S., Chen, K., Zhang, D., Chen, Y., Xu, Y., Liu, J., Wang, X.: and S. Zhuang. Reconfigurable metamaterial for chirality switching and selective intensity modulation. Opt. Express **28**(23), 34804–34811 (2020)
17. ·Z. Li, M., Mutlu, Ozbay, E.: Chiral metamaterials: from optical activity and negative refractive index to asymmetric transmission. J. Opt. **15**(2), 023001 (2013)
18. ·S. Liang, Z., Zhu, Jiang, L.: Twist-angle dependent circular dichroism and related mechanisms in closely stacked Archimedean planar metamaterials. OSA Continuum **4**(4), 1326–1338 (2021)
19. ·H. Liu, Z., Shang, X., Wu, C., Dou, Zhang, J.: Tunable circular dichroism of bilayer b-type chiral nanostructures. Opt. Commun. **448**, 76–81 (2019)
20. ·X. Ma, M., Pu, X., Li, Y., Guo, P., Gao: and X. Luo. Meta-Chirality: Fundamentals, Construction and Applications. Nanomaterials (Basel) **7**(5), 116 (2017)
21. ·X. Ma, Z., Xiao, D., Liu, L., Wang, K., Xu, J., Tang, Wang, Z.: Dispersionless optical activity based on novel windmill-shaped chiral metamaterial. Mod. Phys. Lett. B **30**(04), 1650033 (2016)
22. ·L. Ouyang, W., Wang, D., Rosenmann, D.A., Czaplewski, J., Gao, Yang, X.: Near-infrared chiral plasmonic metasurface absorbers. Opt. Express **26**(24), 31484–31489 (2018)
23. ·E. Prodan, Nordlander, P.: Plasmon hybridization in spherical nanoparticles. J. Chem. Phys. **120**(11), 5444–5454 (2004)
24. ·B. Ranjbar, Gill, P.: Circular dichroism techniques: biomolecular and nanostructural analyses- a review. Chem Biol Drug Des **74**(2), 101–120 (2009)
25. ·A, S., Saadeldin, M.F.O., Hameed, E.M.A., Elkaramany: and S. S. A. Obayya. Highly Sensitive Terahertz Metamaterial Sensor. IEEE Sens. J. **19**(18), 7993–7999 (2019)
26. ·R, S.: Plasmonics in the mid-infrared. Nat. Photonics **6**(7), 409–411 (2012)
27. ·J. Valentine, S., Zhang, T., Zentgraf, E., Ulin-Avila, D.A., Genov, G., Bartal, Zhang, X.: Three-dimensional optical metamaterial with a negative refractive index. Nature **455**(7211), 376–379 (2008)
28. Wang, ·L., Huang, X., Li, M., Dong, J.: Chirality selective metamaterial absorber with dual bands. Opt. Express **27**(18), 25983–25993 (2019)
29. ·Z. Wang, L., Jing, K., Yao, Y., Yang, B., Zheng, C.M., Soukoulis, H., Chen, Liu, Y.: Origami-Based Reconfigurable Metamaterials for Tunable Chirality. Adv. Mater. **29**(27), 1700412 (2017)
30. ·L. Wu, Z., Yang, Y., Cheng, Z., Lu, P., Zhang, M., Zhao, R., Gong, X., Yuan, Y., Zheng, Duan, J.: Electromagnetic manifestation of chirality in layer-by-layer chiral metamaterials. Opt. Express **21**(5),

5239–5246 (2013)

31. ·J. Xu, Y., Fan, R., Yang, Q., Fu, Zhang, F.: Realization of switchable EIT metamaterial by exploiting fluidity of liquid metal. Opt. Express **27**(3), 2837–2843 (2019)
32. ·B. Yan, K., Zhong, H., Ma, Y., Li, C., Sui, J., Wang, Shi, Y.: Planar chiral metamaterial design utilizing metal-silicides for giant circular dichroism and polarization rotation in the infrared region. Opt. Commun. **383**, 57–63 (2017)
33. ·X. Yin, M., Schaferling, B., Metzger, Giessen, H.: Interpreting chiral nanophotonic spectra: the plasmonic Born-Kuhn model. Nano Lett. **13**(12), 6238–6243 (2013)
34. ·X. Yin, M., Schäferling, A.-K.U., Michel, A., Tittl, M., Wuttig, T., Taubner: and H. Giessen. Active Chiral Plasmonics. Nano Lett. **15**(7), 4255–4260 (2015)
35. ·S. Yoo, Park, Q.H.: Metamaterials and chiral sensing: a review of fundamentals and applications. Nanophotonics **8**(2), 249–261 (2019)
36. ·M. Zhang, Q., Lu, Zheng, H.: Tunable circular dichroism created by surface plasmons in bilayer twisted tetramer nanostructure arrays. Journal of the Optical Society of America B **35**(4), 689–693 (2018)
37. Zhang, ·X., Zhang, D., Fu, Y., Li, S., Wei, Y., Chen, K., Wang, X.: and S. Zhuang. 3-D Printed Swastika-Shaped Ultrabroadband Water-Based Microwave Absorber. IEEE Antennas Wirel. Propag. Lett. **19**(5), 821–825 (2020)
38. ·J. Zhou, D.R., Chowdhury, R., Zhao, A.K., Azad, H.-T., Chen, C.M., Soukoulis, A.J., Taylor, and J. F. O'Hara. Terahertz chiral metamaterials with giant and dynamically tunable optical activity. *Physical Review B*, *86*(3) (2012)

Figures

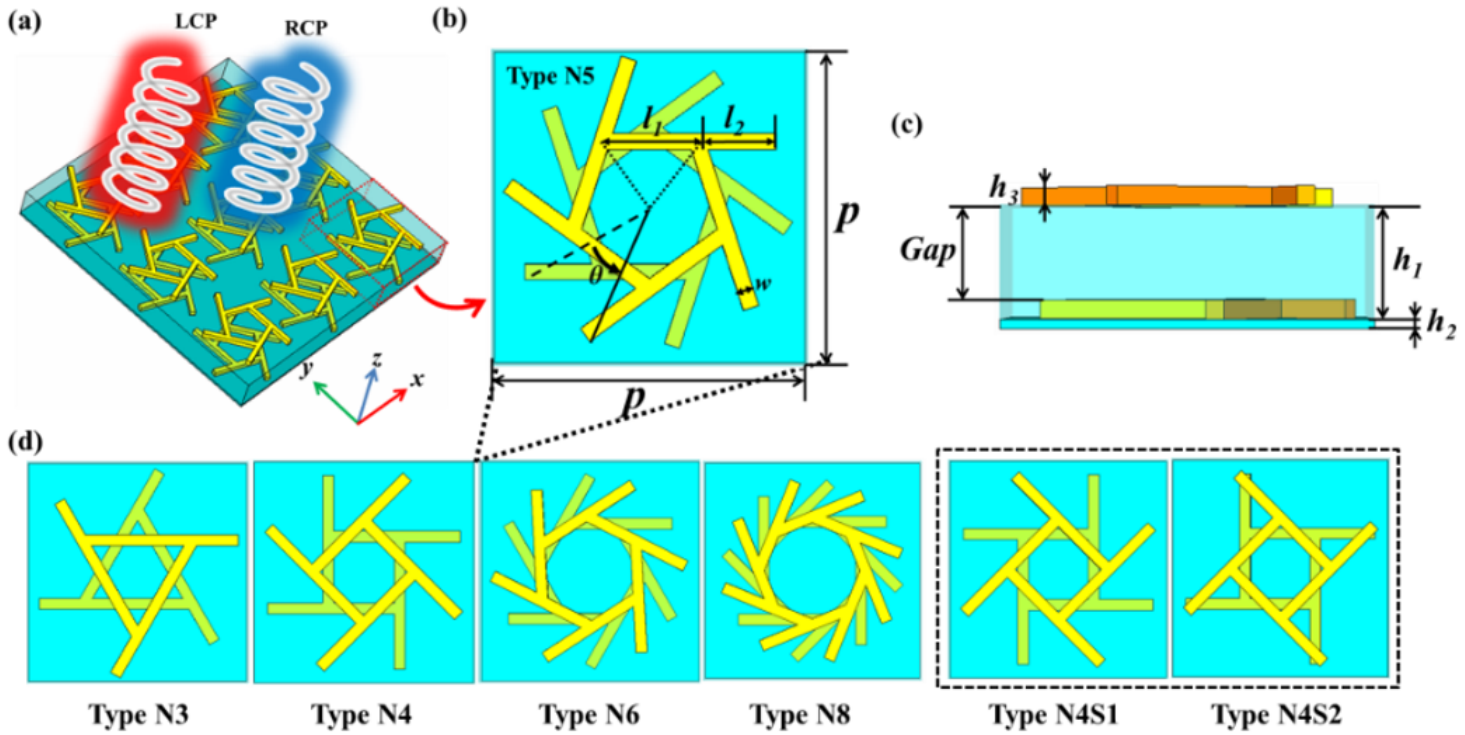

Figure 1

(a) is schematic diagram of metamaterial structure (Type N5); (b) is front view and (c) is side view of one unit with geometric parameters. (d) shows different types of metamaterials which are studied in this paper. Two reconfigure strategies which are applicable to all types are marked by dashed lines. The rotation angles in (b), (c) have been set to 36°; in (d) have been set to 45°.

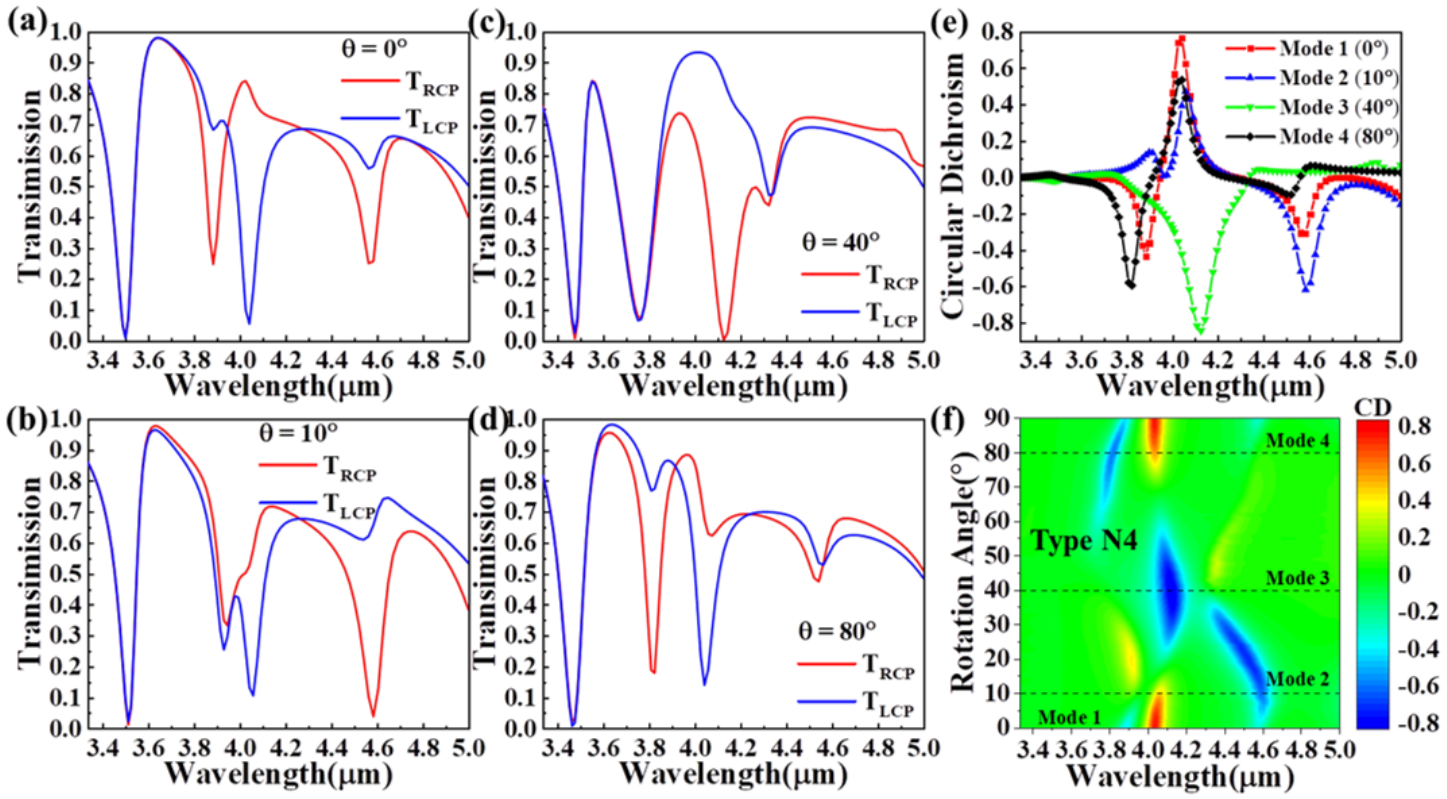

Figure 2

(a)-(d) is transmission spectrum of RCP and LCP waves with rotation angle of 0°, 10°, 40° and 80° respectively (Type N4). (e) is the CD spectra calculated from each transmission spectrum. (f) is the relationship between CD, rotation angles and wavelengths with dash lines marking different modes. It should be noted that Mode 1 is at the 0° coordinate axis.

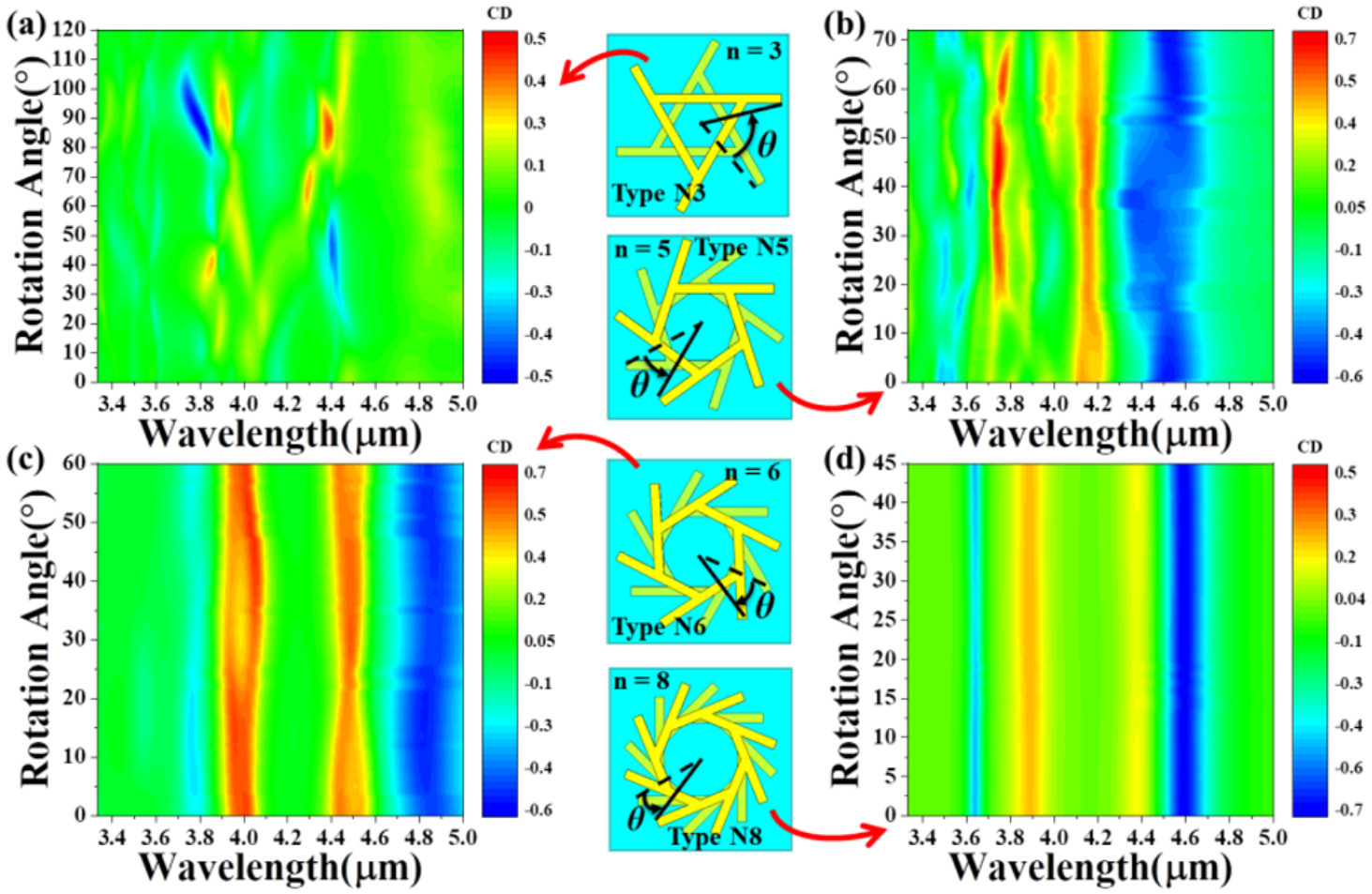

Figure 3

(a), (b), (c), and (d) are the CD spectra of the metamaterial with three, five, six, and eight folds of rotational symmetry respectively. The rotation angle of Type N3, Type N5, Type N6, and Type N8 in the middle of the figure has been set to 60°, 36°, 30°, and 22.5° respectively. The fold of rotational symmetry (n) has been marked in the figure.

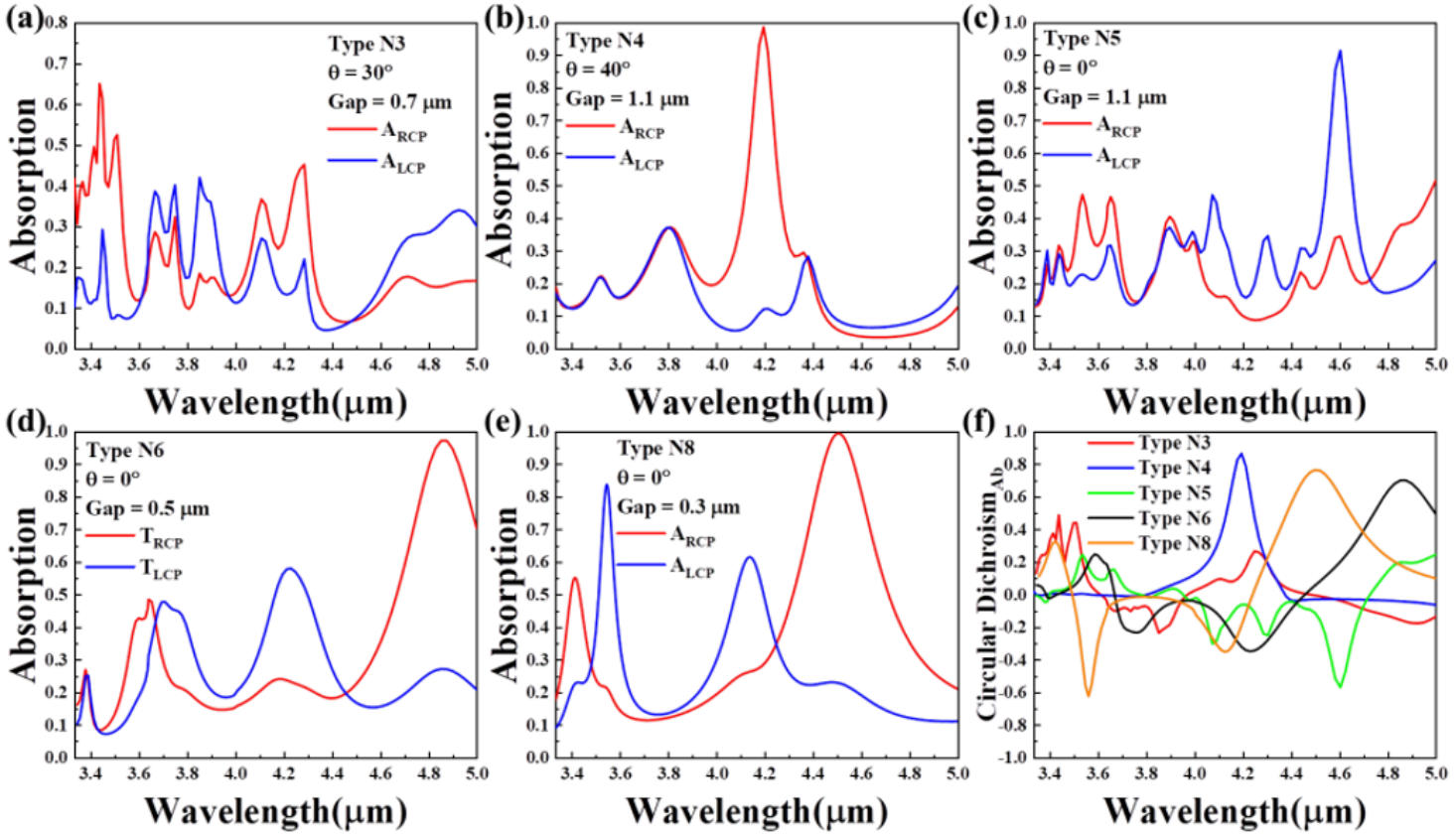

Figure 4

(a)-(e) absorption of different fold of rotational symmetric nano-structures with optimized parameters marked in the figures; (f) is absorptive circular dichroism of (a)-(e).

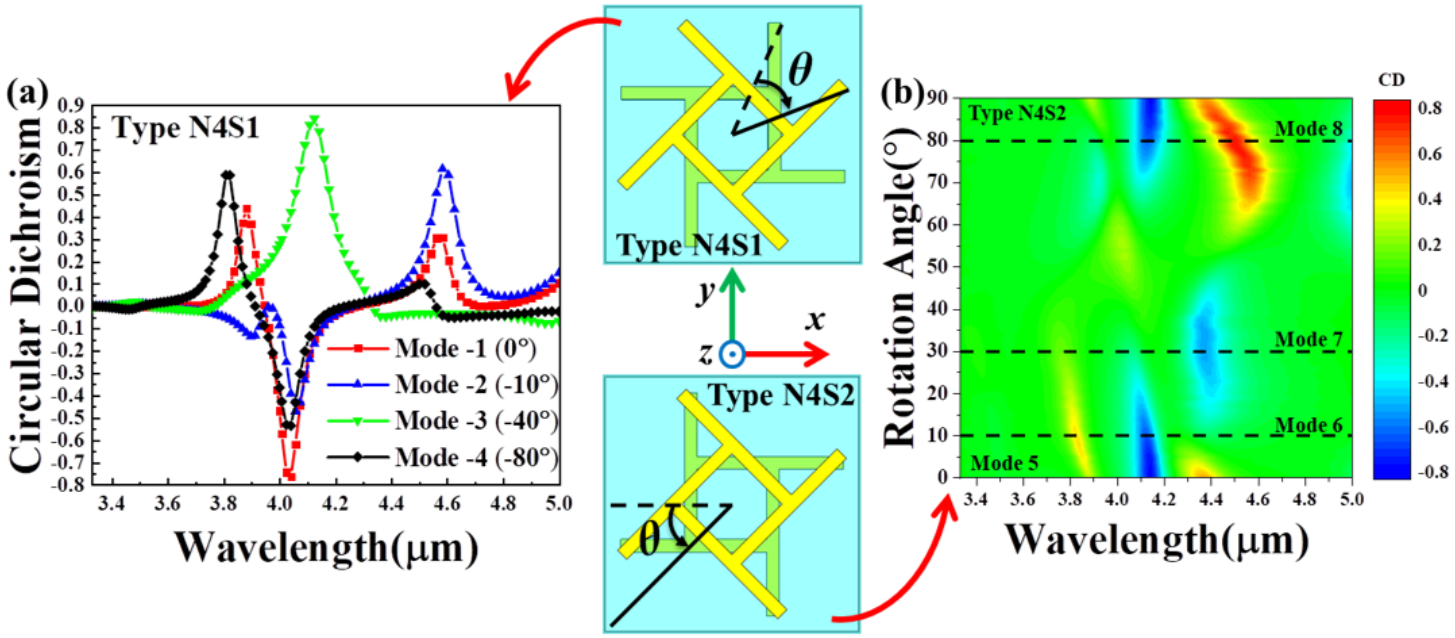

Figure 5

(a) is the CD spectra of Type N4S1; (b) is the contour map of CD spectra, rotation angles, and wavelengths for Type N4S2. The rotation angles of Type N4S1 and Type N4S2 in the middle have been set to -45° and 45°.

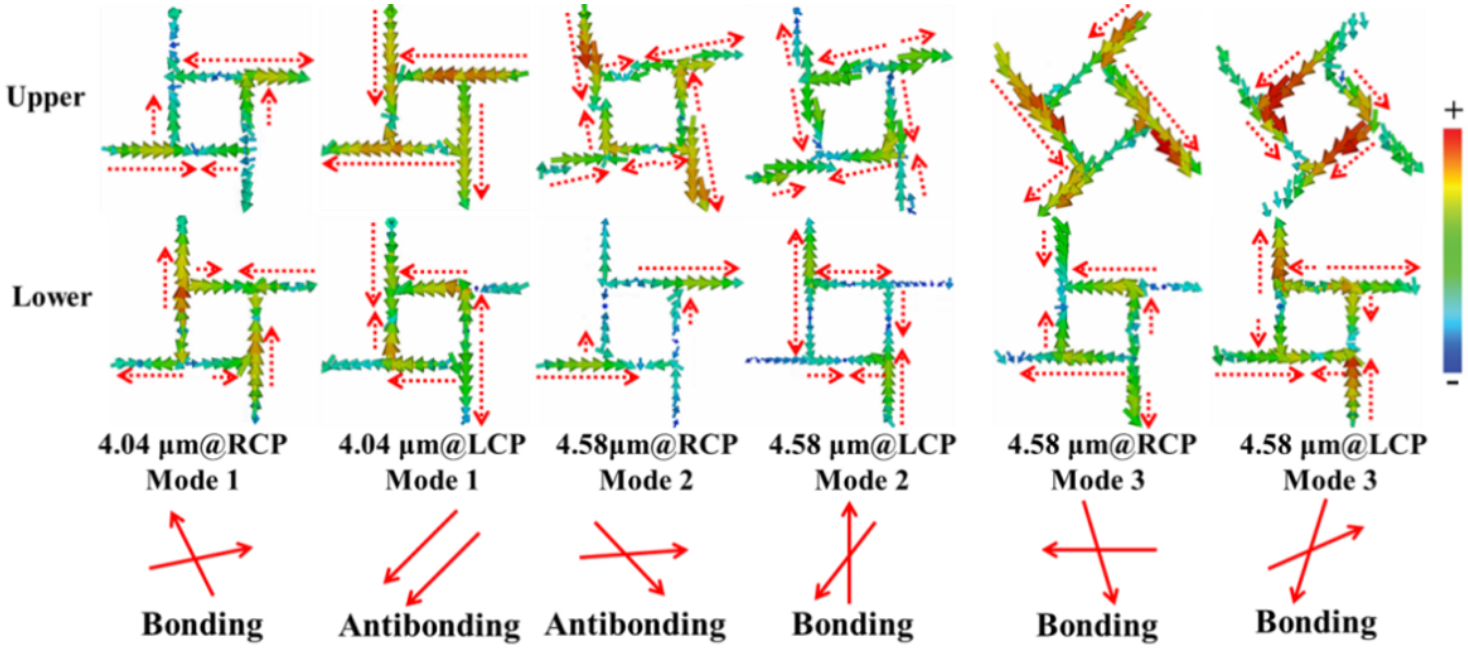

Figure 6

The charge distribution of upper and lower layers at middle and long wavelength bands with Mode 1, Mode 2 and Mode 3 in device Type N4. The red dash line arrows and solid line arrows represent the local electric dipoles and calculated equivalent electric dipoles of two layers.